Enhanced 3D Localization Accuracy of Body mounted Miniature Antennas using Ultra Wideband Technology in Line-of-Sight Scenarios

Manmohan Sharma [1*, 2], Akram Alomainy [2], Clive Parini [3]

[1] School of Electronic Engineering and Computer Science, Queen Mary University of London, London E1 4NS, U.K.
[2] School of Electrical and Electronic Engineering, Nanyang Technological University, Singapore
[*] m.sharma@qmul.ac.uk

Abstract: This paper presents experimental investigations on high precision localization methods of body-worn miniature antennas using ultra-wideband technology in line-of-sight conditions. Time of Arrival data fusion and peak detection techniques are implemented to estimate the three-dimensional location of the transmitting tags in terms of *x*, *y*, *z* Cartesian coordinates. Several pseudo-dynamic experiments have been performed by moving the tag antenna in various directions and the precision with which these slight movements could be resolved has been presented. Some more complex localization experiments have also been undertaken, which involved the tracking of two transmitter tags simultaneously. Excellent 3D localization accuracy in the range of 1-4 cm has been achieved in various experiment settings. A novel approach for achieving sub-centimetre 3D localization accuracy from UWB technology has been proposed and demonstrated successfully. In this approach, the phase centre information of the antennas in a UWB localization system is utilized in position estimation to drastically improve the accuracy of the localization measurements to millimetre levels. By using this technique, the average localization error has been reduced by 86%, 31% and 72% for the *x*, *y* and *z* axes coordinates, respectively.

1. Introduction

Ultra-wideband (UWB) technology has been identified as one of the most promising techniques in future body area networks to enhance a mobile node or a sensor with accurate ranging and tracking capabilities [1], [2]. Impulse-radio ultra-wideband (IR-UWB) systems have, theoretically and practically, much better distance resolution capabilities than any other wireless system. This makes UWB technology ideally suited for localization applications, since the use of very short pulses enables precise time and distance measurement [3], [4]. IR-UWB has the potential to overcome the limitations of current motion tracking technologies and in the near future, will lead to the development of more compact, user-friendly and accurate solutions for motion tracking at reasonable costs. UWB signals do not cause significant interference to other systems operating in the vicinity and do not pose a threat to users' safety as the radiation is non-ionizing and very low-power.

UWB-based localization and tracking has attracted a lot of attention from the research community due to its promising applications in various fields like sports performance analysis, animation, rehabilitation, robotics etc. The benefits of using UWB techniques for achieving high-precision localization as compared to other available technologies has been nicely discussed by Zhang et al. in [5]. Recently published books on UWB communication systems and more general works on wireless networks study UWB positioning techniques too [6]–[8]. Commercially available UWB localization systems and devices such as the ones from Zebra Technologies [9], PLUS [10], Ubisense [11] and Decawave [12] provide a positioning accuracy which is limited to around tens of centimetres. When dealing with tracking of the human motion, the required accuracy is generally in the order of millimetres, especially for application in sports and rehabilitation, which involve tracking fast movements of the limbs [13], [14]. Commercial systems are currently unable to meet such high-precision requirements.

Better localization accuracy from UWB has been documented in the literature. Zwirello et al. presented a UWB-based localization system and attained an average localization accuracy of 2.5 cm [15]. In [16], an accuracy of under 10 cm was achieved in an indoor environment using UWB pulse signals. Fischer et al. reported 3.9 cm localization accuracy by utilizing impulse radio UWB transceivers in [17]. However, all these investigations have only considered localization of tags placed in free-space. The localization accuracy can degrade significantly when the target is to locate tags mounted on the human body. Very limited work is available that could achieve millimetre accuracy using a simple IR-UWB system for 3D localization of on-body tags in realistic environments. The presence of the human body and its effect on the localization accuracy needs to be studied comprehensively as the complex electromagnetic properties of human tissues can significantly affect the characteristics of radio waves.

In this paper, extensive experimental studies involving several 3D localization measurements are presented, and the potential of achieving high-precision localization using ultra-wideband technology in line-of-sight scenarios is demonstrated. Time of arrival data fusion technique is utilized to track the movements of body-mounted miniature UWB transmitters using three Vivaldi antennas as receivers. This paper is an extended version of our preliminary work published in [18]. We

extend our previous work by undertaking comprehensive pseudo-dynamic localization experiments, in which, location of the transmitter tag is estimated while it is being moved in various different directions within the three-dimensional coordinate framework. Experimental campaigns for simultaneous localization of multiple transmitter tags are also carried out and the results from these experiments are provided. In addition, this paper proposes a novel technique for improving the accuracy of UWB-based localization to millimetre-level by making use of antenna phase centre information. A somewhat similar idea of using absolute phase centre to achieve more accurate positioning estimates from GPS antennas was first discussed in [19]. To the best of the authors' knowledge, such a technique of utilizing antenna phase centres for improving the localization accuracy of body-worn nodes based on IR-UWB technology has not been presented in the open literature extensively yet. In addition, very limited work is available that has undertaken a comprehensive experimental analysis to establish the viability and scalability of UWB technology for high-precision 3D localization of on-body tags with millimetre accuracy.

The rest of the paper is organized as follows. Section 2 provides details of the transmitter and receiver antennas, as well as the localization method and experimental setup. In Section 3, results of various three-dimensional localization experiments undertaken in this investigative study are presented. Section 4 describes the proposed technique for achieving millimetre accuracy from UWB-based localization. An experimental analysis regarding the effects of non-line-of-sight scenarios on range estimation between our antennas is provided in Section 5. Lastly, the concluding remarks and key findings of this paper are provided in Section 6.

2. Methodology

2.1. Transmitter and Receiver Antennas

The transmitter antenna utilized for these investigations is a small coplanar waveguide-fed ultra-wideband antenna (Fig. 1*a*). The overall structure of this miniature antenna is 7.9 mm × 16.38 mm in physical dimensions. The antenna is sufficiently compact that it can fit on a fingertip. Therefore, it is ideally suited for wearable applications such as the UWB motion tracking system. Further details about this antenna can be found in [20]. The antenna is much smaller than many other compact antennas such as the ones mentioned in [21], [22], having a similar frequency range. The compact size, wideband characteristics, omnidirectional radiation and decent on-body performance support the suitability of this antenna for wearable UWB applications.

In addition to the miniature UWB transmitter antenna, a wideband Vivaldi antenna was designed to be used as the receiver for the localization measurements. The antenna has an overall size of 28 mm × 40 mm with an FR-4 substrate of 1.6 mm thickness and dielectric constant of 4.3. Both the Vivaldi antenna and the miniature UWB antenna have been designed for operation in the 6 to 10.6 GHz band. The fabricated prototype of the Vivaldi antenna and its design geometry are presented in Fig. 1*b* and 1*c*, respectively.

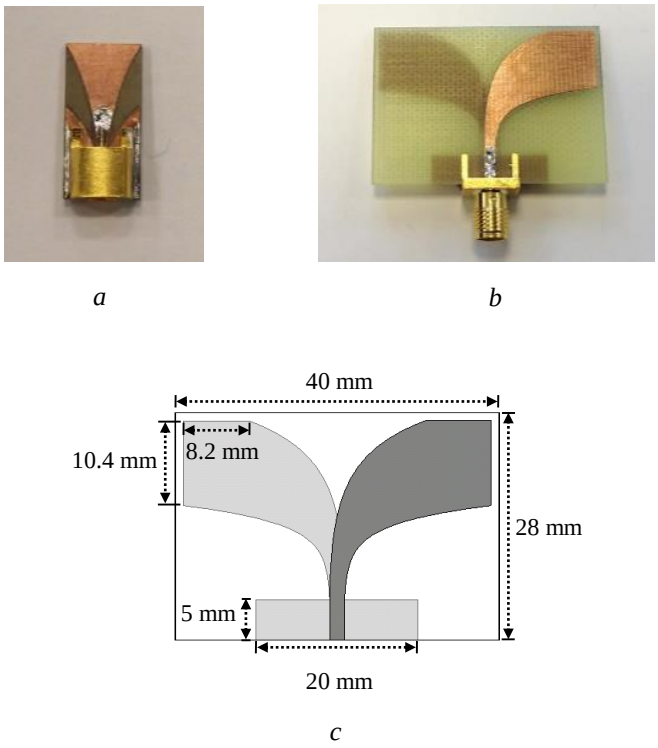

a *b* *c*

Fig. 1. *Antennas used for the localization experiments* **(a)** Miniature UWB antenna fabricated prototype, **(b)** Vivaldi antenna fabricated prototype, **(c)** Vivaldi antenna design geometry

2.2. Localization Method and Measurement Setup

Time of arrival (TOA) measurements estimate the time-of-flight of a signal that travels from one node to the other, thus providing information about the distance between two nodes. Hence, an uncertainty region in the shape of a circle is obtained from TOA measurement at a node. The accuracy of a TOA measurement could be improved by increasing the signal-to-noise ratio (SNR) and/or the effective bandwidth of the signal. As UWB signals have very large bandwidth, this characteristic helps in obtaining highly accurate distance estimation using TOA measurements with the help of UWB radios [23]. TOA-based techniques have been studied extensively in the literature [24]–[27]. In [28], Almazrouei et al. investigated the performance of the TOA method for ranging in indoor channels. Enyang et al. investigated the problem of source localization in wireless sensor networks based on the received signal TOA measurements [29].

The precise estimation of signal TOA is the most significant parameter in microwave-based localization systems. Due to the high time resolution of UWB signals, the range-based TOA approach is one of the most suitable methods for localization in UWB sensor networks [27], [30]. To accurately estimate the TOA of the UWB signal propagating between the transmitter and receiver antenna, channel impulse response and peak detection are employed.

If there are N propagation channels between a transmitter and a receiver (with the amplitude, phase and

delay of the k^{th} path being α_k, φ_k and τ_k respectively), the channel impulse response [31] can be written as

$$y(t) = \sum_{k=1}^{N} \alpha_k e^{j\varphi_k}\, \delta(t - \tau_k) \quad (1)$$

where $\delta(\,)$ is an impulse function. Using the peak detection algorithm, the strongest peak of the channel impulse response is used to obtain an estimate of the signal TOA. The range value based on the estimated signal TOA, which is the one-way propagation time for the signal to travel from the transmitter to the receiver, can be computed by multiplication of the TOA value with the speed of light in air (2.998×10^8 m/s). TOA estimation becomes more challenging for low signal-to-noise ratios and non-line-of-sight situations since the first path (direct line-of-sight path) might not be the strongest path. For such scenarios, the threshold-based leading edge detection technique can be utilized. In this technique, the first point above a defined threshold is declared as the first arriving path and used to determine the TOA. Thus, the selection of an appropriate threshold-level becomes crucial in order to avoid the possibility of too late or too early detection, due to a threshold which is either too high or too low, respectively [32].

For computing the mobile station's unknown coordinates, time of arrival data fusion method [33] was utilized. In this method, the TOA estimates of the mobile transmitter's signal, received by different base stations is combined. The TOA value is multiplied by the speed of light to obtain the range estimate between the mobile transmitter and each of the base station receivers. Determining the location of target node through a set of ranging measurements is then based on trilateration.

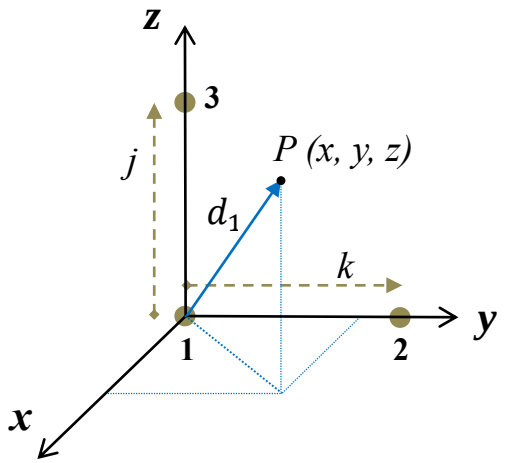

Fig. 2. *The coordinate frame for three-dimensional localization of point P*

Let d_1, d_2 and d_3 denote the range values acquired through three TOA measurements. Then, the following equations will need to be jointly solved, for estimating the location of the mobile station (x, y, z) by means of trilateration:

$${d_i}^2 = (x_i - x)^2 + (y_i - y)^2 + (z_i - z)^2, \quad i = 1,2,3 \quad (2)$$

Here (x_i, y_i, z_i) is the known location of the i^{th} reference node and (x, y, z) is the target node's unknown location. For the coordinate frame shown in Fig. 2, the three equations can be written as follows:

$${d_1}^2 = x^2 + y^2 + z^2 \quad (3)$$

$${d_2}^2 = x^2 + (y - k)^2 + z^2 \quad (4)$$

$${d_3}^2 = x^2 + y^2 + (z - j)^2 \quad (5)$$

The value of y can be computed by subtracting (3) from (4). Thus,

$$y = \frac{{d_1}^2 - {d_2}^2 + k^2}{2k} \quad (6)$$

Similarly z can be computed by subtracting (3) from (5). Thus,

$$z = \frac{{d_1}^2 - {d_3}^2 + j^2}{2j} \quad (7)$$

Hence, by substituting the computed values of y and z into (3) and rearranging the terms, the x-coordinate can be computed:

$$x = \sqrt{{d_1}^2 - y^2 - z^2} \quad (8)$$

The localization measurements involved the usage of three Vivaldi antennas placed in an L-shaped setup, as shown in Fig. 3*a*. Each Vivaldi antenna acted as a base station (BS) receiver and the miniature UWB antenna (placed on a human test subject's finger) as a mobile transmitter whose 3D location had to be estimated. For experimental convenience, the transfer function (S_{21}) is measured between the transmitter and each of the receiver antennas using a four-port Agilent PNA-X. Inverse Fast Fourier Transform (IFFT) is then carried out on the measured transfer function to obtain the channel impulse response. For the line-of-sight communication, channel impulse response peak gives the TOA value, i.e. the time taken by the transmitted signal to propagate to the receiver.

Fig. 3*c* illustrates one such measured sample of the UWB channel impulse response. Here, the peak of the channel impulse response corresponds to a TOA value of around 1.83 nsec. This TOA value when multiplied with the speed of light provides an estimate of the distance between the transmitter and receiver nodes. In this manner, the TOA values thus obtained are multiplied with the speed of light to estimate the distance between the transmitter and each of the three base station receivers. The mobile station's position is then estimated by implementing the data fusion method.

The base station locations were selected before the measurements. BS1 was assumed to be the origin of our 3D coordinate system. BS3 was placed at a horizontal distance of 1 m from BS1. BS2 was kept at a vertical distance of 0.5 m directly above BS1. Hence, by taking BS1 as (0,0,0), the (x, y, z) coordinates of BS2 and BS3 were (0,0,0.5) and (0,1,0) respectively. Location of the mobile station was then

computed in terms of 3D coordinates by using the signal TOA data and the known locations of the three base stations. The feeds of the antennas were used as the reference points to determine their actual positions. Hence the feed port of BS1 was (0,0,0) in the coordinate system and the positions of other base stations and the mobile station position were deduced as the distance of their individual feeds from the BS1 feed. An image of the experimental setup for the localization measurements is illustrated in Fig. 3*b*. The mobile station is placed on the finger of a human test subject and the three fixed base station receivers are in its vicinity.

3. 3D Localization Measurements and Results

This section provides results of the 3D localization experiments undertaken in this investigative study. Numerous localization measurements were carried out by using the body-worn miniature ultra-wideband antennas as transmitters and off-body Vivaldi antennas in the vicinity as the receivers. Experiments have been performed by moving the tag antenna in various directions and the precision with which these slight movements could be resolved has been studied. Some more complex localization experiments were also carried out, involving the tracking of more than one transmitter tag simultaneously. This helps in quantifying the ease with which this system could be scaled up for realizing a full body motion tracking system, having multiple transmitter tags. Moreover, some repeatability measurements were also carried out to measure the variation in the localization results for the same set of measurement scenarios on two different occasions, which helps to assess the reliability and stability of the system.

3.1. Localization of Mobile Tag Being Moved Along the x-axis

For these measurements, the mobile station (MS) was successively shifted away from the plane containing the three base stations, i.e. along the x-axis, in small steps of 10 cm and 3 cm. For both the measurements, the initial distance of the MS was chosen to be 1 m from the plane containing the three base stations. The localization results comparing the actual and estimated positions of the MS from the two measurements are presented in Fig. 4*a* and 4*b*. It can be noticed from the localization results that the position estimation of the MS has been achieved with good accuracy. The 3D coordinates of the MS were estimated with average error values of 3.65 cm, 1.16 cm and 1.15 cm for the x, y and z axes respectively.

It is evident from the above results that the mobile station's gradual motion along the x-axis was resolved very clearly. An interesting phenomenon that was noticed from

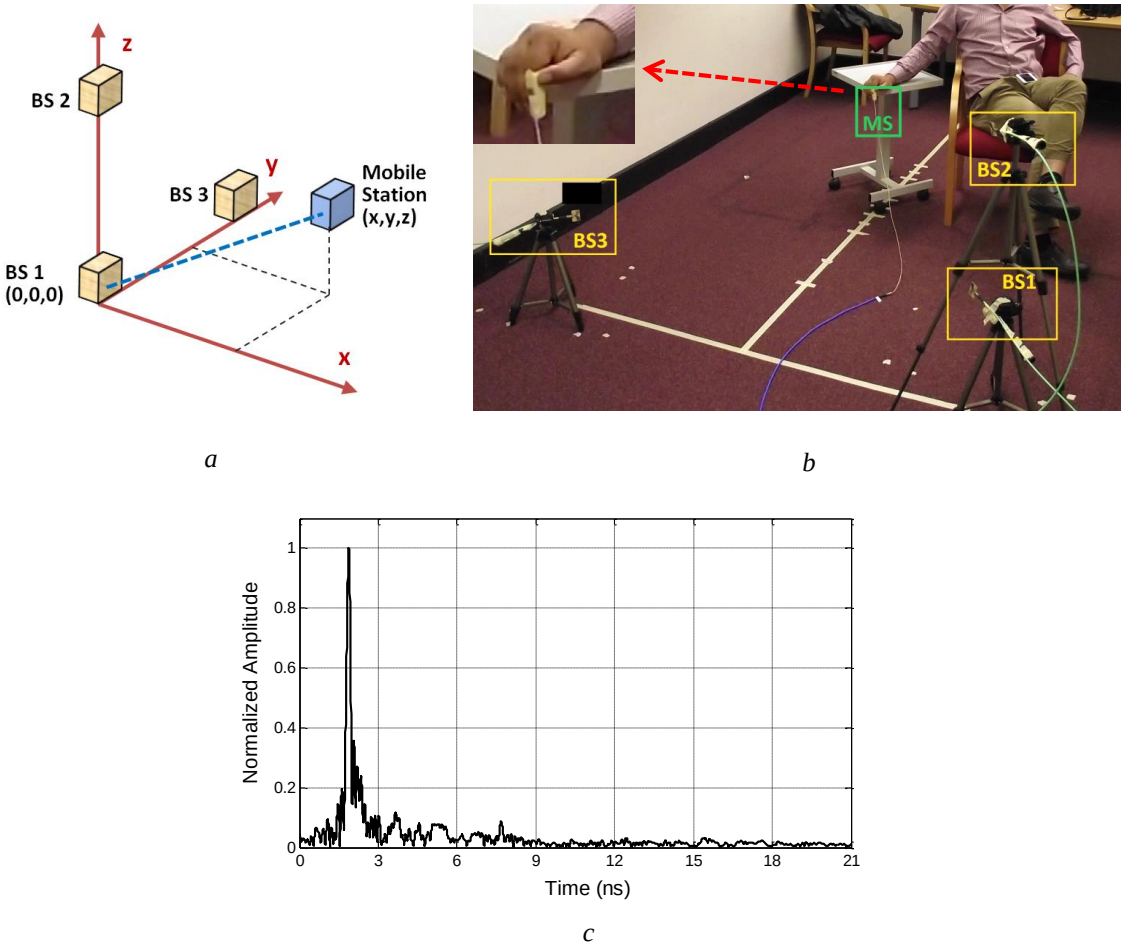

a *b*

c

Fig. 3. *Experimental setup for three-dimensional localization measurements*
(a) The L-shaped measurement configuration of three base stations (BS1-3), **(b)** Illustration of the measurement setup with finger-mounted mobile transmitter (MS) and the three base station receivers (BS1-3). Miniature antenna mounted on the finger is shown in the inset, **(c)** A measured sample of the UWB channel impulse response

the localization results was that there was a consistent shift between the estimated and actual positions of the mobile station. Further localization experiments were carried out to study more about this and how this error could be mitigated.

3.2. Localization of Moving Mobile Tag in the xy and xz planes

For this analysis, the MS was moved in the xy and xz-planes. For the first case, the MS was shifted along the y-axis with increments of 3 cm. Five such measurements were taken, starting with the MS being initially placed 0.7 m away from the plane containing the three BSs. Then the MS was shifted 10 cm further away from the plane containing the three BSs (yz-plane) and the same measurements (with increments of 3 cm in y-axis) were repeated. In this way, four sets of measurements were performed, each having the MS at a specific distance away from the yz-plane for five increments in the y-axis. The results of the localization experiment where the mobile tag was being moved in the xy-plane are presented in Fig. 4*c*. For these measurements, the coordinates of the MS were estimated with average error values of 4.08 cm, 1.32 cm and 1.42 cm for the x, y and z axes respectively.

In a similar manner, another localization experiment was performed where the mobile station was moved in the xz-plane. Here, the MS was shifted with increments of 3 cm vertically (i.e. along the z-axis). Four such measurements were done with the MS placed 0.7 m away from the yz-plane. Then the antenna was shifted 10 cm further away from the plane containing the base stations and the same measurements (with increments of 3 cm in the z-axis) were repeated. In this manner, six groups of localization measurements were performed, each having the MS at a specific distance away from the yz -plane for four increments in z-axis. The localization results for the second experiment have been presented in Fig. 4*d*. For this set of measurements, the coordinates of the MS were estimated with average error values of 4.35 cm, 0.95 cm and 1.62 cm for the x, y and z axes respectively. It can be noticed from Fig. 4*c* and 4*d* that there is a consistent shift in all the estimated positions of the mobile station as compared to the actual positions, exactly as in the localization experiment presented in Section 3.1. When the estimated MS positions

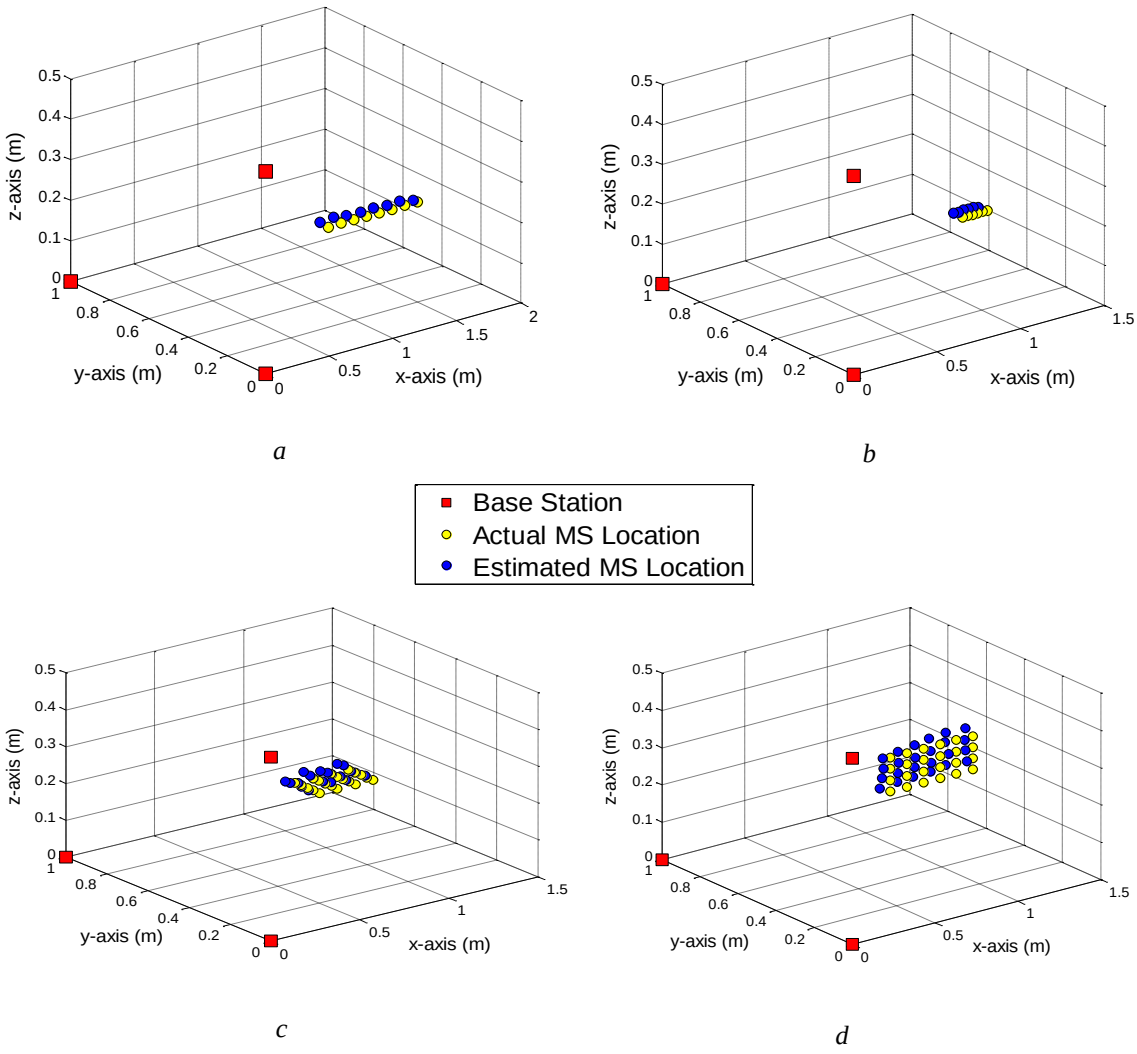

Fig. 4. *Comparison of the actual and estimated locations of the mobile antenna when moved*
(a) Along the *x*-axis with increments of 10 cm, **(b)** Along the *x*-axis with increments of 3 cm, **(c)** In the *xy*-plane, **(d)** In the *xz*-plane

are compared to each other, it can be clearly seen from the plots that the tiny increments of the MS are sensed by the base stations very smoothly and accurately for both the experiments.

3.3. Localization of Two Mobile Tags Simultaneously

For this experiment, two mobile stations were localized simultaneously, both fixed on a human test subject's hand. One MS was attached to the thumb and the other was attached to the index finger. The first measurement was taken with the thumb and index finger fully stretched. The index finger was then slowly brought close to the thumb in five steps, while keeping the thumb position constant. Localization measurements were performed for the thumb location as well as each position of the index finger.

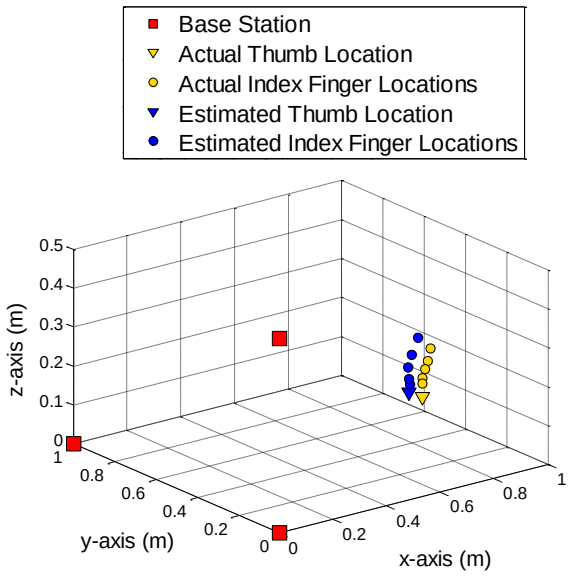

Fig. 5. *Comparison of the actual and estimated locations of two mobile stations fixed on thumb and index finger, being localized simultaneously*

Fig. 5 illustrates the actual and estimated positions of the thumb and the index finger being moved towards the thumb. It can be observed from the figure that the mobile station position on the index finger has been tracked with very good accuracy. The trajectory of the gradual movement of the index finger towards the thumb can be clearly noticed from the figure. However, as noticed in all the previous localization experiments, there is a consistent shift in the estimated positions of the MS as compared to the actual locations. For this experiment, the coordinates of the MS were estimated with average error values of 4.28 cm, 1.31 cm and 1.37 cm for the x, y and z axes respectively.

3.4. Repeatability of the Localization Measurements

In this section, the repeatability of the localization of the mobile tag using the techniques presented in the previous sections of this paper has been examined. The aim of this analysis was to study how the localization results vary for the same measurements repeated on two different occasions, when the measurement environment and all the other parameters were kept unchanged. This investigation helps in assessing the reliability and stability of the UWB-based localization system. For reliable interpretation of fast movements, particularly in the sports applications, there will be a demand for measurements with good repeatability in addition to high accuracy. In this study, four arbitrary locations were chosen for placing the body-mounted mobile tag and these positions were localized through the base station receivers using time of arrival data fusion techniques. A repeat of the four measurements was then carried out to analyse how the estimated locations of the mobile station change when the same measurements are repeated on a second instance. The average difference between the estimated x, y and z coordinates of the first and second set of measurements was 0.67 cm, 0.34 cm and 0.62 cm respectively. This slight difference in repeatability results could be attributed to the movement of the human test subject, since it is really challenging for a real human to remain completely still during these measurements. Nevertheless, this analysis demonstrates that the localization measurements carried out by making use of the ultra-wideband technology are repeatable within a deviation of only a few millimetres.

4. Calibration of Localization Error

From the results of all the localization experiments presented in the previous sub-sections, it was observed that although the small movements of the mobile station were resolved very precisely using the UWB technology, there was a small degree of consistent shift between the estimated and actual positions of the mobile station. Although localization of the MS has been successfully done with average errors mostly in the range of 1-4 cm, the consistency in the magnitude of the error values provides the opportunity to calibrate out this error. By removing the consistent error obtained in the localization measurements, we could potentially achieve sub-centimetre localization accuracy.

Table 1 Average error in estimating coordinates of the MS for various localization experiments

Localization Experiment	Average Error (cm)		
	x	y	z
MS moved along x-axis	3.65	1.16	1.15
MS moved in xy-plane	4.08	1.32	1.42
MS moved in xz-plane	4.35	0.95	1.62
Two MSs localized together	4.28	1.31	1.37
(Overall Average)	4.09	1.19	1.39

The average errors in estimating the x, y and z coordinates of the MS for each of the localization experiments discussed in the previous sections, along with the overall average error values for all the experiments have been summarized in Table 1. It can be observed from these values that the localization error was the least for the y and

z axes for all the experiments as compared to the x-axis. This could be attributed to the fact that all the base stations are situated in the yz-plane, leading to a better localization accuracy for the y and z axes.

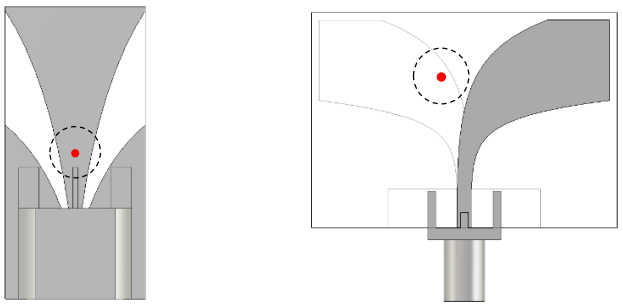

a *b*

Fig. 6. *Simulated phase centres of the antennas at 8.3 GHz frequency*
(a) Miniature UWB antenna, **(b)** Vivaldi antenna

As discussed earlier, the feeds of the antennas were used as the reference points to get the actual and estimated positions of the mobile station. In order to calibrate the error obtained in estimating the MS location and to get more accurate measurement results, the locations of the reference points for localization calculations were adjusted by taking the phase centres of the antennas as the reference points instead. The phase centre of an antenna is described as the apparent point from which the electromagnetic radiation appears to emanate. The offset of the location of the phase centres of the transmitter and receiver antennas was added to the reference points of the antennas that were being used earlier. This meant that the antenna phase centres became the new reference points for our location estimation experiments. These calibrated locations of the base stations were then used to redo the trilateration calculations and the new estimates of the mobile station's locations were thus obtained, which were far more accurate than the earlier location estimates. Making use of the phase centre as the point of reference could actually help in obtaining more accurate estimation of the time-of-flight values and thus ultimately open new avenues towards obtaining high-precision 3D localization from UWB technology. The locations of phase centres of the Vivaldi and the miniature UWB antenna were computed through numerical simulations in CST Microwave Studio software at 8.3 GHz frequency, which is the centre frequency of the 6 to 10.6 GHz target operational band for the antenna system. Fig. 6 shows the positions of the simulated phase centres of the two antennas with respect to the antenna structures.

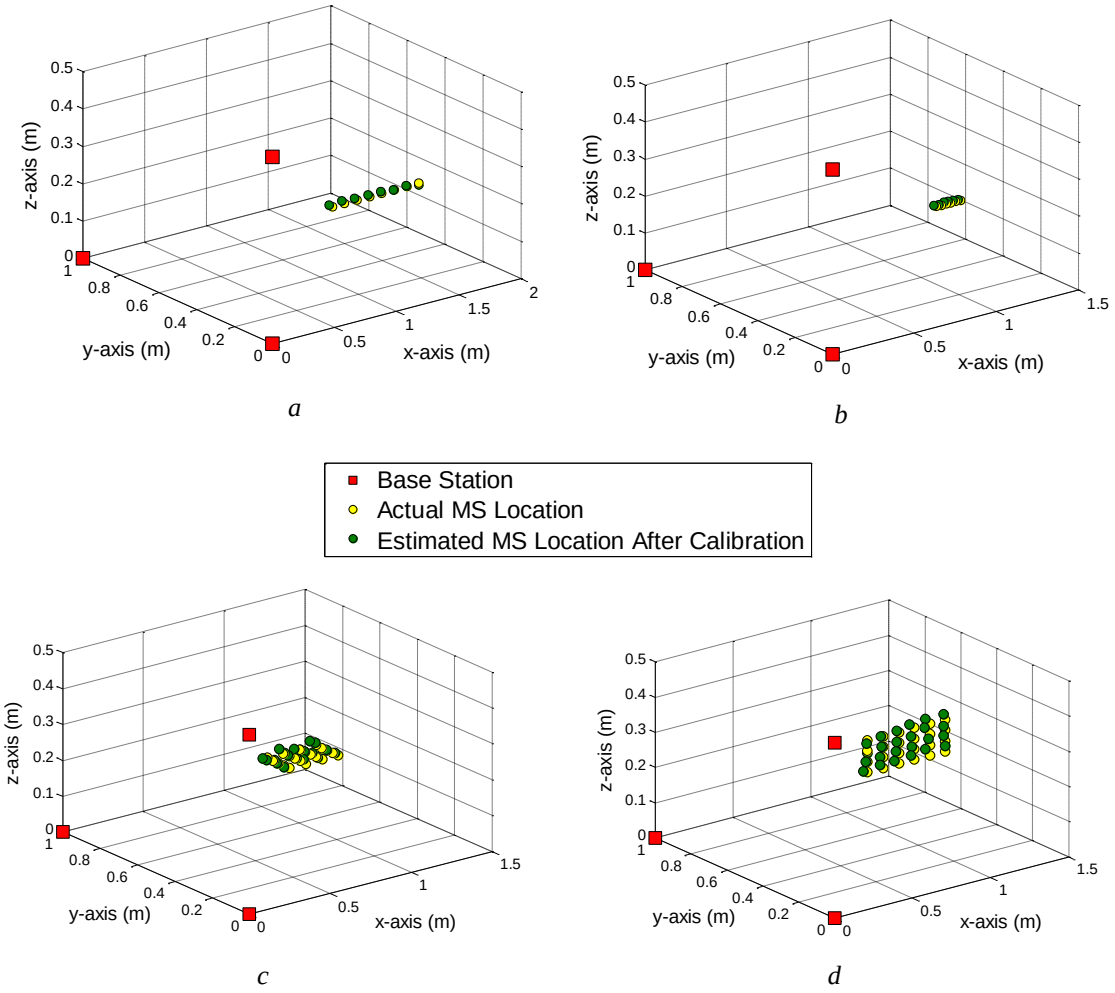

a *b* *c* *d*

Fig. 7. *Actual locations of the mobile station along with its calibrated estimated positions, with the MS being moved*
(a) Along x-axis for increments of 10 cm, **(b)** Along x-axis for increments of 3 cm, **(c)** In the xy-plane, **(d)** In the xz-plane

Fig. 7*a* and 7*b* illustrate estimated locations of the MS after calibration of the average error, along with the actual MS locations, when the MS was being moved along the x-axis. It can be noticed that after calibration, the MS has been localized with a very high precision. After following the calibration procedure, the average error in the estimation of the x, y and z coordinates of the MS was 0.27 cm, 0.84 cm and 0.15 cm respectively. This is in sharp contrast to the localization errors of 3.65 cm, 1.16 cm and 1.15 cm obtained for the x, y and z axes respectively before applying the calibration. Hence, it has been possible to achieve sub-centimetre localization accuracy by taking into consideration the phase centres of the antennas.

The same method of utilizing the antenna phase centres for calibrating out the localization error was repeated for the experiments where the MS was moved in the xy and xz-plane. Fig. 7*c* and 7*d* illustrate the estimated locations of the MS after calibration, along with the actual MS locations, when the MS was being moved in the xy and xz-plane respectively. It can be noticed that after calibration, the positions of the MS have been estimated with very high precision. The average error in estimating the 3D coordinates of the MS for the x, y and z axes became 0.48 cm, 0.69 cm and 0.42 cm, respectively, for movement in the xy-plane and 0.79 cm, 0.77 cm and 0.62 cm, respectively, for movement in the xz-plane. Therefore, once again we have been able to achieve millimetre-level accuracy in localizing the MS by taking into consideration the antenna phase centres as the reference points for determination of the antenna positions. In a similar fashion, the error obtained in the measurements involving localization of two mobile tags simultaneously was also calibrated out. Fig. 8 illustrates the estimated positions of the thumb and the index finger after calibration, along with their actual locations.

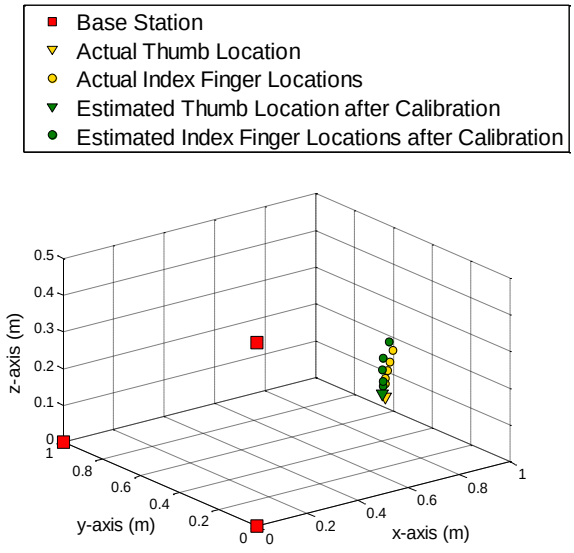

Fig. 8. *Actual locations of thumb and finger mounted mobile stations, along with the calibrated estimated positions*

As observed previously, Fig. 8 demonstrates the advantage of using the antenna phase centres as the reference points in accurately predicting the position of the two mobile stations. Applying the phase centres of the UWB antennas as the reference points, the average error in estimating the 3D coordinates of the two mobile stations for the x, y and z axes becomes 0.69 cm, 0.98 cm and 0.37 cm, respectively. The slightly higher error in the y-axis could be attributed to the dependence of the antenna phase centre on the frequency as well as direction of the received signal. Table 2 provides a summary of the average error values in estimating the x, y and z coordinates of the MS for each of the localization experiments after calibration.

Table 2 Average error in estimating coordinates of the MS after calibration

Localization Experiment	Average Error (cm)		
	x	*y*	*z*
MS moved along *x*-axis	0.27	0.84	0.15
MS moved in *xy*-plane	0.48	0.69	0.42
MS moved in *xz*-plane	0.79	0.77	0.62
Two MSs localized together	0.69	0.98	0.37
(Overall Average)	0.56	0.82	0.39

This approach has demonstrated that millimetre-level localization accuracy could be achieved with UWB technology if the antennas are assumed to be point sources and their phase centres are utilized for obtaining the actual as well as estimated locations. In this way, a major portion of the consistent error being encountered in estimating the MS location could be eliminated. The overall average error for all the above measurements taken as a single set is 0.59 cm. Hence, these investigations have revealed that through taking into consideration the phase centres of the antennas in a positioning system, very precise localization of a target node could be realised.

5. Non-line-of-sight Range Analysis

Although the target application for this work is for motion capture where it is intended that at least three base stations would have a line-of-sight view of a mobile tag, here we briefly consider the effects of non-line-of-sight scenarios. For large obstacles (>10 wavelengths) the error is related to the change in speed of signal propagation through the structure and this is related directly to the relative permittivity of the obstacle. For objects of order a few wavelengths, the propagation time will be a combination of the signal passing through the obstacle and that passing around it, resulting in a more blurred pulse with associated smaller TOA error.

In order to examine the effect of non-line-of-sight communication on the range estimation between the transmitter and receiver antennas, several different types of materials were placed between the two antennas to obstruct their direct line-of-sight path. The four different obstructions used for this analysis were a 0.8 cm thick piece of cardboard, a 1.7 cm thick slab of wood, a sheet of plastic with 0.6 cm thickness and the hand of an adult human test subject. In this experiment, all but the hand can be considered electrically

large. The two antennas were kept at a separation distance of 1 m from each other and the obstructions were placed midway between them for the measurements.

Table 3 Error in range estimates for non-line-of-sight setting between the antennas

Obstruction	Ranging Error (cm)
Cardboard	0.11
Wood	0.54
Plastic	0.30
Human hand	1.92

The error values obtained in estimating the range between the two antennas for each of the four different obstructing materials is provided in Table 3. It was noticed that materials with low relative permittivity had minimal effect on the range estimates between the antennas. The transmitter antenna's radiation was able to pass through these three obstructions, namely wood, plastic and cardboard with delay related directly to the change in relative permittivity. In contrast, the human hand with a significantly high relative permittivity (about 35) had a noticeable effect on the accuracy of the range estimate obtained. A range error of 1.92 cm was observed when the direct line-of-sight path between the antennas was blocked by the human hand. The higher relative permittivity and lossy nature of the human body tissues affect the electromagnetic radiation more profoundly.

6. Conclusion

In this paper, a detailed experimental analysis involving high-precision 3D localization of tiny body-worn antennas through ultra-wideband technology for line-of-sight conditions is presented. Good uncalibrated localization accuracy of 1-4 cm has been achieved through these measurements, with the mobile tag being moved in all the three axes, in a pseudo-dynamic manner. Experimental campaigns with two transmitter tags being localized simultaneously were also undertaken. This analysis helped in quantifying the ease with which such a system could be scaled up for realizing a multi-tag localization system, having numerous transmitter tags being located at the same time. A novel technique for improving the precision of UWB-based localization to realize sub-centimetre accuracy has been proposed and demonstrated successfully. In this technique, the antennas of a UWB localization system are assumed to be point sources and their phase centres are used as reference points for determining the real locations of the nodes and estimating the position of the target mobile nodes. High-precision 3D localization accuracy in the range of 0.4-0.8 cm has been achieved by implementing this novel technique. This amounts to a reduction in the localization error by 86%, 31% and 72% for the x, y and z axes coordinates respectively with the help of this technique. Thus, the feasibility of utilizing UWB technology for high-precision 3D localization has been effectively validated through this investigative study.

7. Acknowledgments

The authors would like to thank Dr. Massimo Candotti, Mr. Deepak Singh Nagarkoti and Mr. Viren Joshi for their assistance with the experimental setup and localization measurements.

8. References

[1] Benedetto, M.G.D., Kaiser, T., Molisch, A.F., *et al.*: 'UWB Communication Systems: A Comprehensive Overview' (Hindawi Publishing Corporation, 2006)

[2] Cao, H., Leung, V., Chow, C., *et al.*: 'Enabling technologies for wireless body area networks: A survey and outlook', IEEE Commun. Mag., 2009, vol. 47, no. 12, pp. 84–93

[3] Crepaldi, M., Paleari, M., Bonanno, A., *et al.*: 'A quasi-digital radio system for muscle force transmission based on event-driven IR-UWB', Proc. IEEE Biomedical Circuits and Systems Conf., Hsinchu, Taiwan, Nov. 2012, pp. 116–119

[4] Fernandes, J.R., Wentzloff, D.: 'Recent advances in IR-UWB transceivers: An overview', Proc. IEEE Int. Symp. on Circuits and Systems, Paris, France, May 2010, pp. 3284–3287

[5] Zhang, D., Xia, F., Yang, Z., *et al.*: 'Localization Technologies for Indoor Human Tracking', Proc. 5th Int. Conf. on Future Info. Technol., Changzhou, China, Oct. 2010, pp. 1–6

[6] Goswami, S., 'Indoor Location Technologies' (Springer, 2013)

[7] Thomä, R., Knöchel, R.H., Sachs, J., *et al.*, 'Ultra-Wideband Radio Technologies for Communications, Localization and Sensor Applications' (InTech, 2013)

[8] Zwick, T., Wiesbeck, W., Timmermann, J., *et al.*, 'Ultra-Wideband RF System Engineering' (Cambridge University Press, 2013)

[9] 'Dart UWB Technology Product Brochure', https://www.zebra.com/content/dam/zebra/product-information/en-us/brochures-datasheets/location-solutions/dartuwb-tech-datasheet-en-us.pdf, accessed 26 November 2016

[10] 'Real Time Location Systems - PLUS Location Systems', http://pluslocation.com, accessed 26 November 2016

[11] 'Ubisense Dimension4', http://ubisense.net/en/products/Dimension4, accessed 26 November 2016

[12] 'DecaWave Product Information: DW1000', http://www.decawave.com/sites/default/files/product-pdf/dw1000-product-brief.pdf, accessed 26 November 2016

[13] Hale, K.S., Stanney, K.M.: 'Handbook of Virtual Environments: Design, Implementation, and Applications' (CRC Press, 2002)

[14] Roetenberg, D.: 'Inertial and Magnetic Sensing of Human Motion'. PhD thesis, Twente University, 2006

[15] Zwirello, L., Schipper, T., Harter, M., *et al.*: 'UWB Localization System for Indoor Applications: Concept, Realization and Analysis', Jour. Electr. Comput. Eng., 2012, vol. 2012

[16] Li, Z., Dehaene, W., Gielen, G.: 'A 3-tier UWB-based indoor localization system for ultra-low-power sensor networks', IEEE Trans. Wirel. Commun., 2009, vol. 8, no. 6, pp. 2813–2818

[17] Fischer, G., Klymenko, O., Martynenko, D., *et al.*: 'An impulse radio UWB transceiver with high-precision TOA measurement unit', Proc. Int. Conf. Indoor Positioning and Indoor Navigation, Zurich, Switzerland, 2010, pp. 1–8

[18] Sharma, M., Alomainy, A., Parini, C.: 'Experimental Investigation of 3D Localisation of an On-body UWB Antenna Using Several Base Stations', Proc. Loughborough Ant. Propag. Conf., Loughborough, U.K., 2014, pp. 173–177

[19] Schmid, R., Steigenberger, P., Gendt, G., et al.: 'Generation of a consistent absolute phase-center correction model for GPS receiver and satellite antennas'. Jour. of Goedesy, 2007, vol. 81, no. 12, pp. 781–798

[20] Sharma, M., Parini, C.: 'A miniature wideband antenna for wearable systems', Proc. Loughborough Ant. Propag. Conf., Loughborough, U.K., 2013, pp. 619–623

[21] Yazdandoost, K.Y., Hamaguchi, K.: 'Very small UWB antenna for WBAN applications', Proc. 5th Int. Symp. Medical Info. and Comm. Technol., Montreux, Switzerland, 2011, pp. 70–73

[22] Chahat, N., Zhadobov, M., Sauleau, R., et al.: 'A compact planar UWB antenna for on-body communications', Proc. 5th Euro. Conf. on Ant. Propag., Rome, Italy, 2011, pp. 3627–3630

[23] Gezici, S., Poor, H.V.: 'Position Estimation via Ultra-Wide-Band Signals', IEEE Spec. Issue on UWB Technol. Emerging Applications, 2009, vol. 97, no. 2, pp. 386–403

[24] Pietrzyk, M.M., Von der Grun, T.: 'Ultra-wideband technology-based ranging platform with real-time signal processing', Proc. 4th Int. Conf. Signal. Process. Comm. Systems, Gold Coast, Australia, Dec. 2010, pp. 1–5

[25] Molisch, A.F.: 'Passive location estimation using TOA measurements', Proc. IEEE Int. Conf. Ultra-Wideband, Bologna, Italy, Sept. 2011, pp. 253–257

[26] Sharp, L., Yu, K.: 'Indoor TOA Error Measurement, Modeling, and Analysis', IEEE Trans. Instrum. Meas., 2014, vol. 63, no. 9, pp. 2129–2144

[27] Bellusci, G., Janssen, G.J.M., Yan, J., *et al.*: 'Performance Evaluation of a Low-Complexity Receiver Concept for TOA-Based Ultrawideband Ranging', IEEE Trans. Veh. Technol., 2012, vol. 61, no. 9, pp. 3825–3837

[28] Almazrouei, E., Al-Sindi, N., Al-Araji, S.R., *et al.*: 'Measurements and characterizations of spatial and temporal TOA based ranging for indoor WLAN channels', Proc. 7th Int. Conf. Signal Process. Comm. Systems, Gold Coast, Australia, Dec. 2013, pp. 1–7

[29] Xu, E., Ding, Z., Dasgupta, S.: 'Source Localization in Wireless Sensor Networks From Signal Time-of-Arrival Measurements', IEEE Trans. Signal Process., 2011, vol. 59, no. 6, pp. 2887–2897

[30] Shen, G., Zetik, R., Yan, H., *et al.*: 'Time of arrival estimation for range-based localization in UWB sensor networks', Proc. IEEE Int. Conf. on Ultra-Wideband, Nanjing, China, Sept. 2010, vol. 2, pp. 1–4

[31] Humphrey, D., Hedley, M.: 'Prior Models for Indoor Super-Resolution Time of Arrival Estimation', Proc. IEEE Veh. Technol. Conf., Barcelona, Spain, Apr. 2009, pp. 1–5

[32] Wehs, T., Leune, T., Cölln, G., *et al.*: 'Detection of distorted IR-UWB pulses in low SNR NLOS scenarios', Proc. IEEE Int. Conf. on Ultra-Wideband, Paris, France, Sept. 2014, pp. 51-56

[33] Sayed, A.H., Tarighat, A., Khajehnouri, N.: 'Network-based wireless location: challenges faced in developing techniques for accurate wireless location information', IEEE Signal Process. Mag., 2005, vol. 22, no. 4, pp. 24–40